ligands, ephrins A2 and A5 in the retina, is involved in this process by modulating EphA receptor function (*20*, *21*). We examined the effect of *Ventroptin* misexpression on the expression patterns of these genes. Overexpression of *Ventroptin* induced expression of *ephrin A2* [which was not expressed in the temporal retina of the control eye (Fig. 4B, a)] in the temporal retina mainly in ganglion cells (Fig. 4B, b; 6 out of 6 embryos); whereas we did not detect any obvious alteration in the expression patterns of *EphA3* and *ephrin A5* (*10*). The ectopic projection of the dorsal and dorsotemporal axons to the caudal end of the tectum is explained by this *ephrin A2* induction: *Ephrin A2* overexpression in the retina possibly modified the signal transduction capacity of EphA receptors to make them insensitive to ephrins in the posterior tectum (*20*). *CBF-1*, *CBF-2*, *SOHo1*, and *GH6* are known to be involved in the retinal specification along the A-P axis and show asymmetric distributions along the A-P axis in the retina far earlier than *Ventroptin* (*3*, *6*). *Ventroptin* misexpression did not alter the expression patterns of these transcription factors (*10*). On the other hand, *SOHo1* and *GH6* do not affect the expression of *ephrin A2* (*6*), which suggests that *Ventroptin* is not controlled by these two factors.

The polarity along the D-V axis in the retina appears to be determined after stage 11 and before stage 13/14 in the chick (*22*, *23*). *BMP-4* and *Ventroptin* expressions are detectable in the optic vesicle from stage 10 or 11 onward (*5*, *10*). Therefore, the counteraction between Ventroptin and BMP-4 appears to determine and maintain the regional specificity along the D-V axis. At E6, when the first retinal axons enter the tectum (*24*), *Ventroptin* shows the nasal high–temporal low gradient expression pattern. From this stage on, Ventroptin seems to control retinotectal projection along the A-P axis by controlling the expression of *ephrin A2*. *BMP-4* is expressed specifically in the dorsal retina, evenly along the A-P axis. At later stages (E6 to 8), expression of *BMP-4* was markedly reduced and was detected only in the peripheral margin of the retina (*10*). Thus, BMP-4 is not likely to be involved in the projection along the A-P axis. On the other hand, we found that Noggin, a structurally unrelated BMP antagonist, had the same activity as Ventroptin in expression of *Tbx5* (*10*), *cVax* (*10*), and *ephrin A2* (Fig. 4B, c; 6 out of 6 embryos), when it was misexpressed in the retina. These results suggest the presence of another member of the TGF-β family in the retina, which binds to Ventroptin (and Noggin) and is involved in retinotectal projection along the A-P axis. Our study thus indicates that BMP family members and Ventroptin are involved in topographic retinotectal projection along the D-V and A-P axes.

References and Notes

1. R. W. Sperry, *Proc. Natl. Acad. Sci. U.S.A.* **50**, 703 (1963).
2. G. A. Hyatt *et al.*, *Development* **122**, 195 (1996).
3. J. Yuasa, S. Hirano, M. Yamagata, M. Noda, *Nature* **382**, 632 (1996).
4. D. Schulte, T. Furukawa, M. A. Peters, C. A. Kozak, C. L. Cepko, *Neuron* **24**, 541 (1999).
5. K. Koshiba-Takeuchi *et al.*, *Science* **287**, 134 (2000).
6. D. Schulte, C. L. Cepko, *Development* **127**, 5033 (2000).
7. R. Suzuki *et al.*, *Mech. Dev.* **98**, 37 (2000).
8. Supplementary Web material is available on *Science* Online at www.sciencemag.org/cgi/content/full/293/5527/111/DC1.
9. H. Suzuki *et al.*, *Nucleic Acids Res.* **24**, 289 (1996).
10. H. Sakuta *et al.*, data not shown.
11. A. J. Kahn, *Dev. Biol.* **38**, 30 (1974).
12. A. T. Dudley, E. J. Robertson, *Dev. Dyn.* **208**, 349 (1997).
13. Chick *Ventroptin* was also expressed in the forebrain and diencephalon (*10*). It was also expressed in limb buds, with similar expression patterns in both the wing and leg buds (*10*). The expression patterns of *Ventroptin* in these organs were also complementary to that of *BMP-4*. Therefore, Ventroptin may also control the morphogenesis of the brain and limbs in cooperation with other BMP-neutralizing factors. *Ventroptin* expression was not detectable in the spinal cord at E8 (*10*).
14. W. C. Smith, *Trends Genet.* **15**, 3 (1999).
15. A. Fainsod, *et al.*, *Mech. Dev.* **63**, 39 (1997).
16. I. L. Blitz, O. Shimmi, K. Wunnenberg-Stapleton, M. B. O'Connor, K. W. Cho, *Dev. Biol.* **223**, 120 (2000).
17. In embryos with misexpressed *Ventroptin*, the dorsonasal axons also projected to the posterior end of the dorsal tectum (3 out of 3 embryos). On the other hand, the ventral axons, in which *Ventroptin* is endogenously expressed at a significant level, projected to the normal places (4 out of 4 embryos) (*10*).
18. H. J. Cheng, M. Nakamoto, A. D. Bergemann, J. G. Flanagan, *Cell* **82**, 371 (1995).
19. B. Monschau *et al.*, *EMBO J.* **16**, 1258 (1997).
20. M. R. Hornberger *et al.*, *Neuron* **22**, 731 (1999).
21. D. Dutting, C. Handwerker, U. Drescher, *Dev. Biol.* **216**, 297 (1999).
22. W. J. Crossland, W. M. Cowan, L. A. Rogers, J. P. Kelly, *J. Comp. Neurol.* **155**, 127 (1974).
23. T. Matsuno, N. Itasaki, H. Ichijo, H. Nakamura, *Neurosci. Res.* **15**, 96 (1992).
24. W. J. Crossland, W. M. Cowan, L. A. Rogers, *Brain Res.* **91**, 1 (1975).
25. We thank S. Takami, M. Gotoh, S. Tsukada, M. Ishida, H. Kuribayashi, and S. Usami for technical assistance and A. Kodama for secretarial assistance. Supported by grants from the Ministry of Education, Science, Sports and Culture of Japan, and from Core Research for Evolutional Science and Technology of the Japan Science and Technology Corporation.

18 December 2000; accepted 4 June 2001

A Transcriptively Active Complex of APP with Fe65 and Histone Acetyltransferase Tip60

Xinwei Cao and Thomas C. Südhof*

Amyloid-β precursor protein (APP), a widely expressed cell-surface protein, is cleaved in the transmembrane region by γ-secretase. γ-Cleavage of APP produces the extracellular amyloid β-peptide of Alzheimer's disease and releases an intracellular tail fragment of unknown physiological function. We now demonstrate that the cytoplasmic tail of APP forms a multimeric complex with the nuclear adaptor protein Fe65 and the histone acetyltransferase Tip60. This complex potently stimulates transcription via heterologous Gal4- or LexA-DNA binding domains, suggesting that release of the cytoplasmic tail of APP by γ-cleavage may function in gene expression.

Amyloid-β precursor protein is a cell-surface protein with a large NH_2-terminal extracellular sequence, a single transmembrane region (TMR), and a short COOH-terminal cytoplasmic tail (*1–4*). The α- and β-secretases initially cleave APP at defined extracellular sequences outside of the TMR. Thereafter, γ-secretase cuts APP in the middle of the TMR to generate small extracellular peptides and an intracellular fragment that is composed of half of the TMR (10 to 12 residues) and the cytoplasmic tail (47 residues). The small secreted peptides include amyloid-β peptides (Aβ40 and Aβ42), which are involved in Alzheimer's disease. γ-Cleavage of APP requires presenilins, intrinsic membrane proteins that are mutated in some cases of familial Alzheimer's disease (*1–5*). In addition to APP, two closely related homologs, APLP1 and APLP2, are expressed in vertebrates and also appear to be cleaved by α- and γ-secretases (*6*). The structures of APP and APLPs resemble cell-surface receptors whose proteolysis may be triggered by an external ligand; indeed, several binding activities of the extra- and intracellular regions of APP have been identified [e.g., see (*7–10*)]. Furthermore, triple knockouts of APP, APLP1, and APLP2 in mice are lethal, suggesting that these proteins are essential (*11*). However, the function of APP and APLPs, and of their proteolytic cleavages, remains unclear. Clues to such a function come from

---

The Center for Basic Neuroscience, Department of Molecular Genetics, and Howard Hughes Medical Institute, The University of Texas Southwestern Medical Center, Dallas, TX 75390–9111 USA.

*To whom correspondence should be addressed. E-mail: Thomas.Sudhof@UTSouthwestern.edu

Notch proteins, cell-surface receptors that are also cleaved in the TMR in a presenilin-dependent reaction (*12–14*). Cleavage of Notch proteins liberates a cytoplasmic fragment that regulates nuclear transcription (*15*, *16*), raising the possibility that cleavage of APP may have an analogous role.

To examine a possible function for APP in transcription, we constructed fusion proteins of APP with the DNA binding domains of yeast transcription factor Gal4 (*17*) or bacterial transcription factor LexA (*18*). We engineered Gal4 and LexA into the intracellular tail of full-length APP_{695} at the cytoplasmic boundary of the TMR or fused them to the NH_2-terminus of the isolated cytoplasmic tail. The two distinct DNA binding domains (Gal4 and LexA) were used in these experiments in order to avoid sequence-specific artifacts. We transfected the APP-Gal4 and APP-LexA fusion proteins into PC12, HEK293, COS, or HeLa cells, and measured transactivation of transcription from cotransfected Gal4- and LexA-dependent reporter plasmid expressing luciferase (*19*, *20*). Isolated Gal4 and LexA were used as negative controls, and all cells were cotransfected with a constitutive β-galactosidase expression plasmid to standardize the transfection efficiency. Little transactivation was observed with the APP-Gal4 and APP-LexA fusion proteins over Gal4 or LexA alone (about fivefold; Fig. 1, A and B). Thus, the cytoplasmic tail of APP, when overexpressed in cells as a fusion protein with a heterologous DNA binding domain, does not greatly stimulate transcription by itself, suggesting that APP may require binding of a cofactor. To search for such cofactors, we performed yeast two-hybrid screens for proteins that bind to the cytoplasmic tail of APP (*21*). Similar to previous screens (*7–9*), Fe65 was the major interacting protein identified, although it was isolated at an unexpectedly high frequency (90% of all clones).

We then tested whether binding of Fe65 to APP could activate transcription. Cotransfecting Fe65 with the APP-Gal4 and APP-LexA fusion proteins greatly stimulated transcription (e.g., >2000-fold over Gal4 in HeLa cells), suggesting that Fe65 is a potent transactivator (Fig. 1, A and B). Strong transactivation by Fe65 was observed in all cell lines tested (PC12, HEK293, COS, or HeLa cells), whereas Mintl/X11, which also binds to the cytoplasmic tail of APP (*9–14*), had no significant effect (Fig. 1C). Neither Fe65 nor Mintl/X11 affected transcription of the control β-galactosidase plasmid cotransfected into all cells. Because Fe65 stimulated transcription even when Gal4 or LexA was inserted into full-length APP, the APP fusion proteins appear to be cleaved in the transfected cells. Immunoblotting revealed that in transfected COS cells, the size of the APP-Gal4 cleavage products corresponds precisely to those of the α- and γ-cleavage products of APP, indicating that APP is cleaved correctly by γ-secretase (*22*) and that the hydrophobic NH_2-terminal sequence in the γ-cleavage product does not inhibit nuclear translocation.

In the cytoplasmic tail of APP, Fe65 binds to the NPTY sequence (*8*, *9*, *23*). To test whether binding of Fe65 to APP mediates transactivation, we mutated the NPTY sequence to NATA. As shown by yeast two-hybrid assays and coimmunoprecipitations, this mutation abolished Fe65 binding (*22*). The same mutation also abolished the Fe65-dependent stimulation of transcription (Fig. 1, A and B). Furthermore, when we replaced the cytoplasmic tail of APP-Gal4 with that of neurexin 1 (*24*), Fe65 was unable to stimulate transactivation (about twofold induction; Fig. 1D). However, when we transplanted 32 amino acids from the cytoplasmic tail of APP containing the NPTY sequence into the neurexin cytoplasmic tail, potent transactivaton by Fe65 was recovered (>200-fold induction). These results are consistent with the notion that Fe65 potentiates transcription by directly binding to APP-Gal4 and APP-LexA.

The Fe65 multidomain protein is composed of a negatively charged NH_2-terminal sequence with no homology to other proteins, a central WW domain, and two COOH-terminal PTB domains, the PTB1 and PTB2 domains (*8*, *9*). The negatively charged NH_2-terminal sequences of Fe65 stimulates Gal4-dependent transcription (*25*), the PTB1 domain binds to the transcription factor CP2/LSF/LBP1 (*26*), and the PTB2 domain interacts with the cytoplasmic tail of APP (*8*, *9*). As an initial approach to elucidating how Fe65 activates transcription, we examined a series of Fe65 deletion mutants (*27*). Transactivation assays with these mutants showed that the WW domain and both PTB domains of Fe65 are essential for stimulating transcription, independent of the DNA binding domain used (Fig. 2). By contrast, deletion of the NH_2-terminal third of Fe65 with the acidic region suspected of activating transcription (*25*) had no effect. In addition to deletions, we used point mutations in the WW domain to assess the precise need for the WW domain in transactivation. Substitution of one of the conserved tryptophan residues of the WW domain of Fe65 did not impair transactivation, but replacement of the central YYW motif with alanine residues abolished transactivation (Fig. 2). Immunoblotting con-

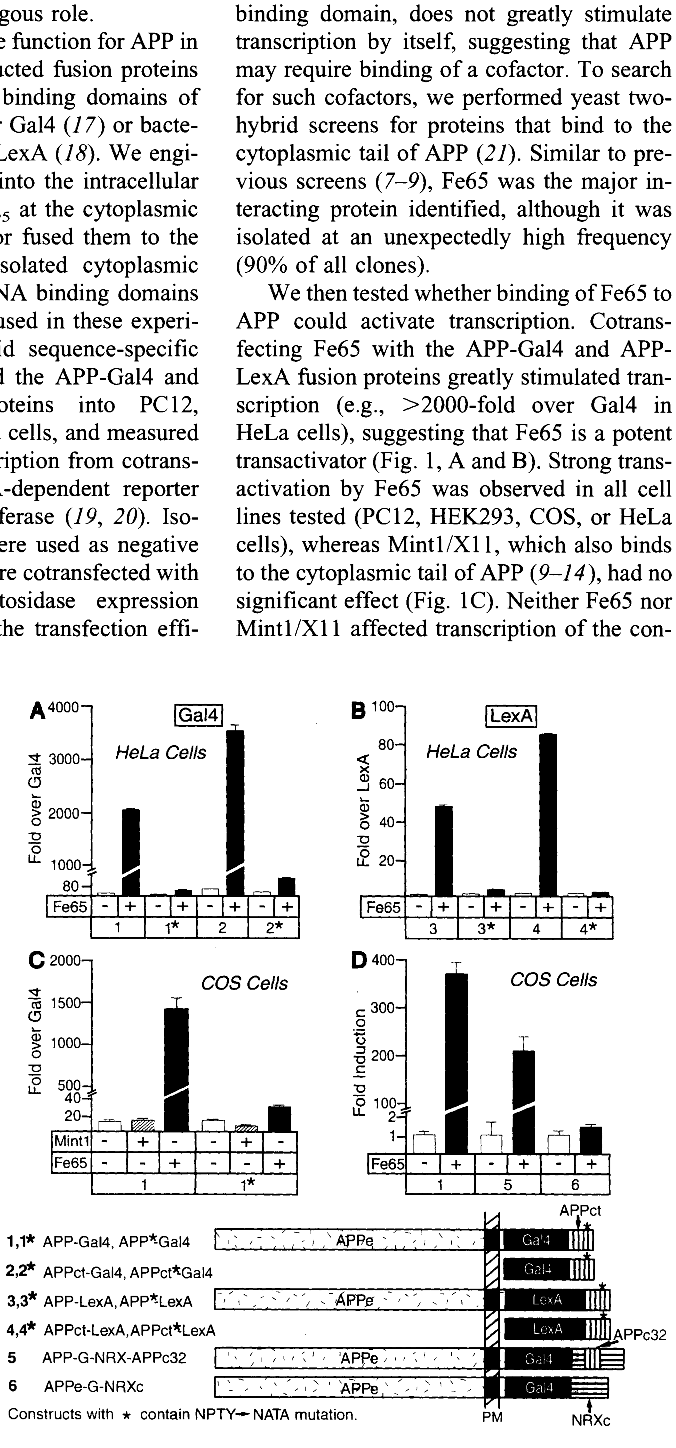

Fig. 1. Fe65 potently stimulates transcription mediated by APP proteins fused to Gal4 or LexA DNA binding domains. (**A** to **D**) Results of transactivation assays obtained with the constructs schematically displayed below the panels. Diagrams exhibit representative experiments in which cells were cotransfected with a Gal4- or LexA-luciferase reporter plasmid (to measure transactivation), a β-galactosidase plasmid (to normalize for transfection efficiency), and the test plasmids identified by numbers below the bars. Constructs marked with an asterisk contain a point mutation in the NPTY sequence of the APP cytoplasmic tail that inactivates Fe65 binding. (A and B) Potent transactivation of transcription is achieved with APP-fusion proteins of both Gal4 and LexA DNA binding domains only when Fe65 is present. (C) This effect is specific for Fe65 because another binding protein to the APP cytoplasmic tail, Mint1/X11, does not achieve stimulation. (D) The Fe65-binding site in the APP cytoplasmic tail confers onto an unrelated sequence (the neurexin cytoplasmic tail) the property of transactivation. Note inhibition of stimulation by mutation of the Fe65-binding site in all instances. The normalized luciferase activity is expressed as fold induction over transcription by Gal4 or LexA alone (A to C), or as fold induction over APP-Gal4 alone (D). Similar results obtained with COS, HEK293, PC12, and HeLa cells (*47*).

firmed that mutant Fe65 proteins were stably expressed, and immunoprecipitations showed that mutants still interacted with APP as long as the PTB2 domain was present, suggesting that the Fe65 mutants were not inactive because of instability or of inability to bind to APP (*22*). Thus all three canonical domains of Fe65 (the WW domain and the two PTB domains) likely have to interact with target molecules in stimulating transcription.

In order to activate transcription, Fe65 presumably interacts with DNA binding proteins, histone acetyltransferases, and general transcription factors. A candidate binding partner for Fe65 is the transcription factor LBP/CP2/LSF, which was reported to bind to the PTB1 domain of Fe65 (*26*). However, we observed only a weak interaction between LBP/CP2/LSF and Fe65 in yeast two-hybrid assays and detected no change in transactivation when we cotransfected LBP/CP2/LSF with Fe65 and APP-Gal4 (*27*). Therefore, we searched for other potential Fe65-interacting proteins using yeast two-hybrid screens. We identified a single prey clone that strongly bound to the PTB1 domain of Fe65 (*28*). This clone encodes Tip60, a histone acetyltransferase that is expressed in two alternatively spliced forms [Tip60α and β (*29*, *30*)]. Tip60 is part of a large nuclear protein complex that contains structural DNA binding, ATPase, and DNA helicase activities in addition to histone acetyltransferase activity (*31*, *32*). Quantitative yeast two-hybrid assays and glutathione *S*-transferase (GST) pull-down assays confirmed a strong interaction of Fe65 with rat and human Tip60 proteins [Fig. 3, A to C (*28*, *33*)]. GST-Tip60 efficiently pulled down APP together with Fe65; conversely, a GST-fusion protein of the APP cytoplasmic tail captured Tip60 together with Fe65, suggesting that the APP cytoplasmic tail, Fe65, and Tip60 form a stable trimeric complex in vitro (Fig. 3, B and C).

Although PTB domains usually bind to NPXY sequences, variant binding sequences have also been observed (*34*, *35*). In a search for a possible PTB domain target sequence in Tip60, we detected a single motif that is remotely similar to the NPXY sequence (NKSY; residues 257 to 260). Mapping of the NKSY sequence onto the three-dimensional structure of Esa1, a related yeast histone acetyltransferase (*36*), suggests that the NKSY sequence is located on a surface loop of a conserved domain, and thus it is accessible for a binding partner. To test whether the PTB1 domain of Fe65 binds to this site, we mutated the Tip60 NKSY sequence into NASA. No binding of Fe65 was observed for the mutant as measured either by quantitative yeast two-hybrid assays or GST pull-down assays (Fig. 3, A and B), suggesting that the PTB1 domain of Fe65 binds to the NKSY sequence in Tip60.

We next examined the localizations of APP, Fe65, and Tip60 in transfected cells [Fig. 4 (*37*)]. When expressed alone, Fe65 and Tip60 are colocalized in the nucleus as reported previously (*29*–*32*, *38*). APP probed with an antibody to the cytoplasmic tail exhibits a diffuse vesicular distribution, consistent with the fact that the majority of APP is uncleaved and probably localizes to recycling vesicles. Upon cotransfection of wild-type APP with Fe65 and Tip60, most Fe65 shifts to the same location as APP, presumably because it binds to uncleaved APP in cytoplasmic vesicles (Fig. 4). When Fe65 is co-

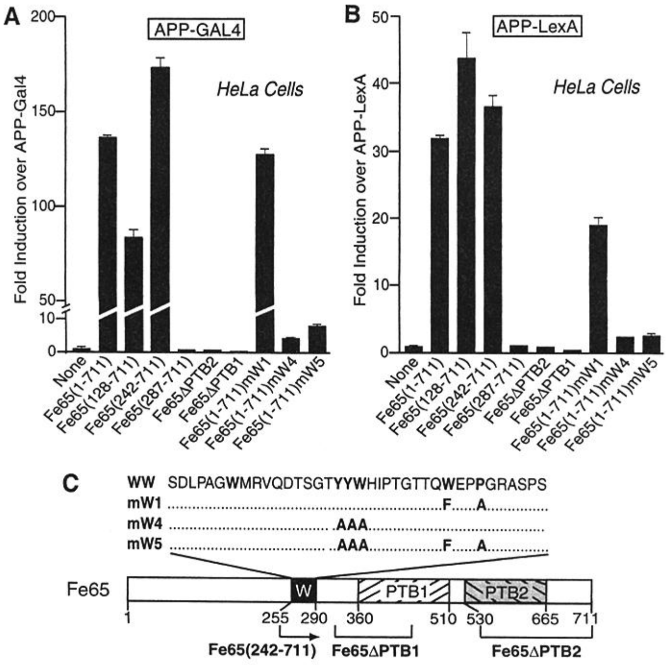

Fig. 2. The WW domain and both PTB domains of Fe65 are required for stimulation of transactivation. (**A** and **B**) Full-length APP-Gal4 and APP-LexA fusion proteins were cotransfected with Gal4- or LexA-reporter plasmids, β-galactosidase control plasmid, and the various Fe65 expression plasmids as indicated. The resulting transactivation is expressed in fold induction over transfection with APP-Gal4 or APP-LexA alone. (**C**) Domain structure of Fe65 with residue numbers of domain boundaries. The sequences of the point mutants in the WW domain are shown above the diagram, and the locations of the deletion mutants used in (A) and (B) are displayed below the diagram.

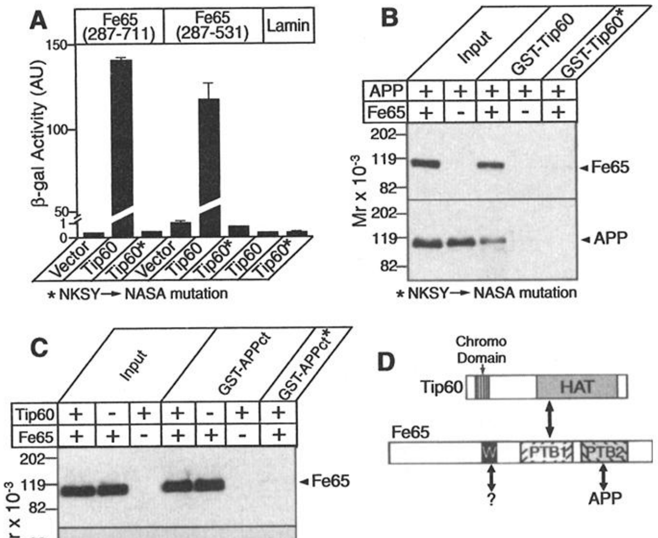

Fig. 3. Histone acetyltransferase Tip60 binds to Fe65 and forms a multimeric complex with Fe65 and the cytoplasmic tail of APP. (**A**) Quantitative yeast two-hybrid assays of Fe65 binding to wild-type rat Tip60 (residues 63 to 454) and mutant Tip60 (Tip60*) in which the NKSY sequence in a loop of the histone acetyltransferase domain (residues 257 to 260) was mutated to NASA. The Fe65-bait vectors encode either both PTB domains or only the PTB1 domain; a lamin bait vector was used as negative control as indicated above the bar diagram. (**B** and **C**) GST pull-down assays with wild-type and mutant GST-Tip60 (B) or wild-type and mutant GST-APP cytoplasmic tail (C). Proteins from COS cells cotransfected with Myc-Fe65 (128-711) and APP (B) or Myc-Fe65 (128-711) and HA-Tip60 (C) were used for GST pull-down experiments, and bound proteins were analyzed by immunoblotting with antibodies to Myc-Fe65 (128-711), APP, and HA-Tip60, as indicated. (**D**) Domain structures of Tip60 and Fe65, and locations of their interacting sequences. Tip60 contains an NH_2-terminal chromo domain and a COOH-terminal histone acetyltransferase (HAT) sequence that includes the NKSY sequence required for binding to Fe65.

expressed with mutant APP that is unable to bind Fe65, it resumes a largely nuclear localization. In contrast, Tip60 was always present in the nucleus (Fig. 4). Together these data suggest that overexpressed APP binds to Fe65 so strongly that it captures most of the Fe65 in the cytoplasm, indicating that Fe65 can move between nucleus and cytoplasm. We did not detect significant staining for APP in the nucleus, possibly because the fraction of APP that is cleaved is very small, and because the cytoplasmic APP fragment produced may be unstable, as previously observed for Notch proteins (*12–16*).

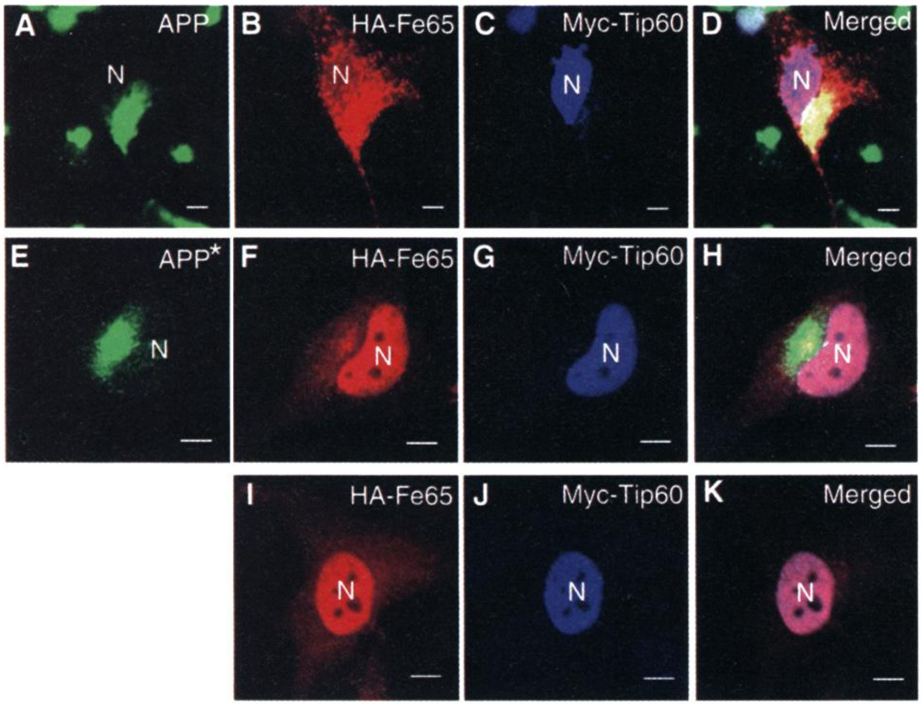

Fig. 4. Localization of Fe65, Tip60, and APP in transfected HeLa cells. (**A** to **D**) Triple-labeling of cells coexpressing APP (green), Fe65 (red; labeled by an NH_2-terminal HA tag) and Tip60 (blue; labeled by an NH_2-terminal Myc tag). (**E** to **H**) Triple-labeling of cells as in (A to D), except that mutant APP (APP*), which is unable to bind Fe65, was transfected. (**I** to **K**) Localization of Fe65 and Tip60 in cells not expressing APP. Note that Tip60 is concentrated in the nucleus (N) under all conditions. In contrast, Fe65 is nuclear in the absence of APP or in the presence of mutant APP*, but largely relocalized to the cytoplasm by wild-type APP. Because of limited sensitivity, the apparent lack of nuclear staining for APP does not exclude the possibility that a fraction of APP (<5%) is localized to the nucleus. Calibration bars, 10 μm.

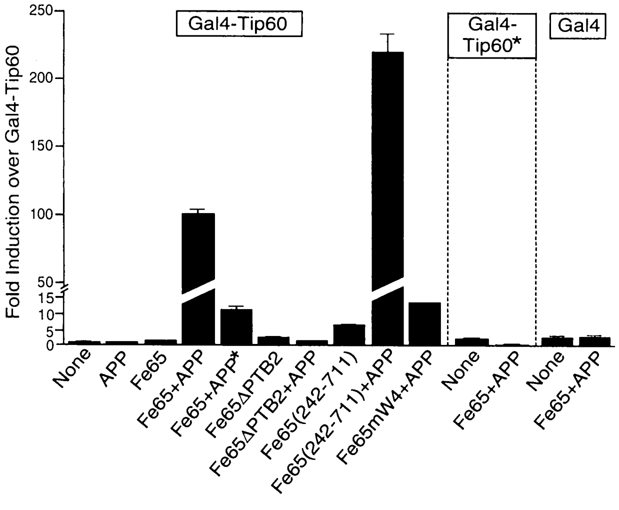

Fig. 5. Fe65 and APP are required for transactivation of Gal4-Tip60. Gal4-fusion proteins with full length human wild-type Tip60 (Gal4-Tip60), mutant Tip60 (Gal4-Tip60*), or Gal4 alone were cotransfected into COS cells with a Gal4-reporter plasmid, a β-galactosidase control plasmid, and the indicated APP and Fe65 expression plasmids. The mutant Tip60 used carries a point mutation that inactivates Fe65 binding (see Fig. 3). Cotransfected Fe65 proteins include deletions of the PTB2 domain, which binds APP (Fe65ΔPTB2), and a point mutation in the WW domain that inactivates the ability of Fe65 to stimulate APP-Gal4 mediated transcription (Fe65mW4). The APP mutant used (APP*) is unable to bind Fe65. Note that Gal4-Tip60 transactivation depends on the presence of both wild-type APP and Fe65.

The interaction of Tip60 with Fe65 is potentially important for the transcriptional activation mediated by Fe65 because it couples Fe65 to the Tip60 complex and thus directly links Fe65 to transcriptional regulation. Our observations could be explained by at least two models that imply different functions for APP in Fe65-dependent transcriptional activation. The first model suggests that the physiological role of APP is to keep Fe65 out of the nucleus, and that γ-cleavage of APP liberates Fe65 for a nuclear function. According to this model, Fe65 transactivates APP-Gal4 or APP-LexA, because it latches Fe65, Tip60, and other nuclear proteins onto the heterologous DNA binding domains that are artificially fused to APP. The second model, by contrast, suggests that the cytoplasmic tail of APP normally functions in transcription when it is bound to nuclear Fe65, and that the cytoplasmic tail of APP released by γ-cleavage has a direct function in transcription. According to the second model, Fe65 stimulates APP-Gal4– or APP-LexA–mediated transcription because APP has a direct function in transcription independent of a heterologous DNA binding domain. Both models link γ-cleavage of APP to transcriptional activation, but assign different roles for the released cytoplasmic tail in transcriptional activation.

To differentiate between these models, we constructed a Gal4-Tip60 fusion protein, and tested the effects of Fe65 and APP on Gal4-dependent transactivation [Fig. 5 (*39*)]. Gal4-Tip60 alone was unable to support significant Gal4-dependent transcription (no activation over Gal4 alone). Expression of either Fe65 or APP alone with Gal4-Tip60 did not enhance transactivation. However, when we coexpressed Gal4-Tip60 with both Fe65 and APP, transactivation was stimulated dramatically (~100-fold; Fig. 5). Mutant APP that is unable to bind to Fe65 (APP*) was largely inactive (~10-fold enhancement). Furthermore, little transactivation was observed when Fe65 and APP were coexpressed with mutant Gal4-Tip60 (Gal4-Tip60*) which is unable to bind to Fe65, or with Gal4 only. As described above, Fe65-dependent stimulation of transactivation by APP-Gal4 and APP-LexA proteins requires all three canonical Fe65 domains (the WW domain and the two PTB domains) (Fig. 2). To test whether the same applies for the Fe65- and APP-mediated transactivation of Gal4-Tip60, we examined Fe65 mutants in this assay (Fig. 5). As expected, the NH_2-terminal sequence of Fe65 was not needed for potentiating Gal4-Tip60–dependent transactivation, whereas the PTB2 domain that binds to APP was essential. The WW domain of Fe65 was also essential, indicating that Fe65 interacts with additional factors besides Tip60 and APP in stimulating transactivation. Together these data suggest that the cytoplasmic tail of APP has a direct active role in stimulating transactivation and that it collaborates with Fe65 in enhancing transcription by Gal4-Tip60.

APP is physiologically processed by α- or β-secretases followed by γ-secretase (*1–4*). However, the orderly and regulated degradation of APP has been a puzzling phenomenon ever since it was initially described because it has no apparent biological benefit. We now report three observations that link γ-cleavage of APP to transcriptional activation. First, we show that the cytoplasmic tail of APP forms a multimeric complex with Fe65, a multidomain adaptor protein (*8*, *9*), and Tip60, a histone acetyltransferase that functions in chromatin remodeling, DNA repair, and transcription (*31*, *32*). Second, we demonstrate that APP fused to DNA binding domains from yeast Gal4 or bacterial LexA exhibits only weak transcriptional activity (about fivefold over Gal4 alone) but is dramatically stimulated by Fe65 (>2000-fold in the case of APP-Gal4). This stimulation requires intact binding sites for APP and for Tip60 in Fe65 and a functional WW domain in Fe65. Third, we find that Gal4-Tip60 is transcriptionally inactive by itself but can be potently transactivated upon coexpression of APP and Fe65. Both APP and Fe65 are required, and any mutation that disrupts the complex of Fe65 with the APP cytoplasmic tail and with Tip60 abolishes this effect.

The most parsimonious explanation for these observations is that the complex of Fe65 with the cytoplasmic tail of APP directly acts in transcription when bound to Tip60. However, several alternative hypotheses are also possible. For example, APP may initiate a nuclear signal without participating in transcription, although this seems less likely in view of the fact that Tip60 and Fe65 can form a direct complex with the cytoplasmic tail of APP. A direct function of the cytoplasmic tail of APP in transcription would agree remarkably well with that of Notch proteins (*15*, *16*). The proposed similarity between APP and Notch provides evidence for a general role of presenilin-dependent proteolysis in regulating transcription (*40*, *41*). According to this hypothesis, cytoplasmic tails of cell-surface proteins are released by presenilin-dependent proteolysis so that they can then regulate transcription. In spite of this similarity, however, the upstream regulation of proteolysis and the downstream target transcription factors are distinct and place APP and Notch into different functional contexts.

The proposed function of APP and its homologs may help to explain why double or triple knockouts in these proteins are lethal (*11*), and why overexpression of COOH-terminal APP-fragments is cytotoxic (*42*, *43*). However, the current studies have limitations that must be overcome before a function for APP in transcription is assured. Our experiments were performed with chimeric proteins containing exogenous DNA binding domains (LexA and Gal4). If the APP-Fe65-Tip60 complex physiologically regulates transcription, it must be coupled to an endogenous DNA binding protein that remains to be identified. This DNA binding protein may be a component of the Tip60 complex that exhibits DNA binding activity (*32*), or it may interact with the WW domain of Fe65. Furthermore, all of the current experiments were performed in transfected cells. It will be necessary to demonstrate that endogenous proteins perform similar functions, which will require identification of endogenous genes that are activated by the complex. In addition, demonstration that the cytoplasmic tail of APP normally enters the nucleus, which was also long elusive for Notch, is still lacking. Finally, Notch cleavage is regulated by ligand binding (*15*, *16*), suggesting that APP cleavage may also be regulated. Because regulation of APP cleavage will not only control the release of the cytoplasmic tail but also secretion of amyloid β-peptides, this regulation could be important in Alzheimer's disease. Thus, insight into how APP cleavage is regulated represents another major goal of future research. The approaches and observations described in the current study may be helpful for these objectives that will not only be important for knowledge of the normal function of APP, but also for the pathogenesis of Alzheimer's disease.

References and Notes

1. D. J. Selkoe, *Trends Cell Biol.* **8**, 447 (1998).
2. T. A. Bayer, R. Cappai, C. L. Masters, K. Beyreuther, G. Multhaup, *Mol. Psychiatry* **4**, 524 (1999).
3. C. Haass, B. De Strooper, *Science* **286**, 916 (1999).
4. D. L. Price, R. E. Tanzi, D. R. Borchelt, S. S. Sisodia, *Ann. Rev. Genet.* **32**, 461 (1998).
5. M. S. Wolfe *et al.*, *Nature* **398**, 513 (1999).
6. S. Naruse *et al.*, *Neuron* **21**, 1213 (1998).
7. F. Fiore *et al.*, *J. Biol. Chem.* **270**, 30853 (1995).
8. D. M. McLoughlin, C. C. Miller, *FEBS Lett.* **397**, 197 (1996).
9. J. P. Borg, J. Ooi, E. Levy, B. Margolis, *Mol. Cell. Biol.* **16**, 6229 (1996).
10. M. Z. Kounnas *et al.*, *Cell* **82**, 331 (1995).
11. S. Heber *et al.*, *J. Neurosci.* **20**, 7951 (2000).
12. Y. Ye, N. Lukinova, M. E. Fortini, *Nature* **398**, 525 (1999).
13. B. De Strooper *et al.*, *Nature* **398**, 518 (1999).
14. G. Struhl, I. Greenwald, *Nature* **398**, 522 (1999).
15. E. H. Schroeter, J. A. Kisslinger, R. Kopan, *Nature* **393**, 382 (1998).
16. G. Struhl, A. Adachi, *Cell* **93**, 649 (1998).
17. H. Kakidani, M. Ptashne, *Cell* **52**, 161 (1988).
18. G. M. Smith *et al.*, *EMBO J.* **7**, 3975 (1988).
19. PC12, COS, HeLa, and HEK293 cells were cotransfected at 50 to 80% confluency in 6-well plates using Fugene6 (Roche), and 3 to 5 plasmids [1.0 to 3.0 μg DNA per well, depending on cell types; see plasmid list in (*22*) for description of all constructs]. All transfections included (i) Gal4 (pG5E1B-luc) or LexA (pL8G5-luc) reporter plasmids; (ii) constitutively expressed β-galactosidase expression plasmid (pCMV-LacZ); (iii) the Gal4- or LexA-fusion protein vectors; and (iv) some transfections included one or two additional plasmids that encode cofactors. Cells were harvested 48 hr posttransfection in 0.2 ml per well reporter lysis buffer (Promega), and their luciferase and β-galactosidase activities were determined with the Promega luciferase assay kit and the *O*-nitrophenyl-D-galacto-pyranoside method, respectively. The luciferase activity was standardized by the β-galactosidase activity, and normalized for the transactivation observed in cells expressing Gal4 or LexA alone. Values shown are averages of transactivation assays carried out in duplicate, and repeated at least three times for each cell type and constructs. Most constructs were assayed in three or four cell lines, but only representative results for one cell line are shown. To confirm expression of transfected proteins and secretase cleavage of the various APP constructs, transfected cells were also analyzed by immunoblotting using antibodies to the respective proteins and/or antibodies to the epitope tags attached to the proteins.
20. For transactivation by APP-Gal4 and APP-LexA constructs, cells were cotransfected with one of the following: (i) pG5E1B-luc (Gal4 reporter plasmid) or pL8G5-luc (LexA-reporter plasmid); (ii) pCMV-LacZ (β-galactosidase control plasmid); (iii) pMst (Gal4), pMst-APP (APP-Gal4), pMst-APP* (APP*-Gal4), pMst-APPγ (APPγ-Gal4), pMst-APPγ* (APPγ*-Gal4), pMst-AN-APPc32 (APP-G-NRX-APPc32), pMst-AN (APPe-G-NRXc), pML (LexA), pML-APP (APP-LexA), pML-APP* (APP*-LexA), pML-APPct (APPct-LexA), pML-APPct* (APPct*-LexA); and (iv) pCMV-Mint1 (Mint1) or pCMV5-Fe65 (Fe65) where indicated. Analyses were performed as described in (*19*).
21. A yeast two-hybrid cDNA library in pVP16-3 was screened with pBTM116-APP encoding the cytoplasmic tail of human APP_{695} as described (*44*, *45*). Of 80 positive clones, 72 encoded Fe65 and one Fe65-like protein. The full-length rat Fe65 sequence has been submitted to GenBank (accession number AF333983). Interactions were quantified using liquid β-galactosidase assays on yeast strains harboring various bait and prey clones (*22*).
22. Supplementary material is available on *Science* Online at www.sciencemag.org/cgi/content/full/293/5527/115/DC1.
23. Single-letter abbreviations for the amino acid residues are as follows: A, Ala; C, Cys; D, Asp; E, Glu; F, Phe; G, Gly; H, His; I, Ile; K, Lys; L, Leu; M, Met; N, Asn; P, Pro; Q, Gln; R, Arg; S, Ser; T, Thr; V, Val; W, Trp; Y, Tyr; and X, any amino acid.
24. Y. A. Ushkaryov, A. G. Petrenko, M. Geppert, T. C. Südhof, *Science* **257**, 50 (1992).
25. A. Duilio *et al.*, *Nucleic Acids Res.* **19**, 5269 (1991).
26. N. Zambrano, G. Minopoli, P. de Candia, T. Russo, *J. Biol. Chem.* **273**, 20128 (1998).
27. For transactivation assays of Fe65 mutants, cells were cotransfected with one of the following: (i) pG5E1B-luc (Gal4 reporter plasmid) or pL8G5-luc (LexA-reporter plasmid); (ii) pCMV-LacZ (β-galactosidase control plasmid); (iii) pMst (Gal4), pMst-APP (APP-Gal4), pML (LexA), or pML-APP (APP-LexA); and (iv) pCMV5-Fe65 (Fe65), pCMVMyc-Fe65(128-711) [Fe65(128-711)], pCMVMyc-Fe65(242-711) [Fe65(242-711)], pCMVMyc-Fe65(287-711) [Fe65(287-711)], pCMV5-Fe65(1-553) (Fe65ΔPT B2), pCMVMyc-Fe65Δ PTB1 (Fe65Δ PTB1), pCMV5-Fe65mW1(Fe65mW1), pCMV5-Fe65mW2 (Fe65mW2), pCMV5-Fe65mW3 (Fe65mW3), pCMV5-Fe65mW4 (Fe65mW4), or pCMV5-Fe65mW5 (Fe65mW5), where indicated. In addition, plasmid pCS2+MT-SEF encoding Myc-tagged full-length human LBP-1c (1 to 450 residues) was cotransfected in some experiments. Analyses were performed as described in (*19*); plasmids are described in (*22*).
28. Yeast two-hybrid screens were carried out with a rat Fe65 fragment (residues 287 to 711) as described in (*21*) and (*22*). Out of 100 clones analyzed, 9 clones encoded APLP1, and 8 clones Tip60β (residues 63 to 454 of the insert-minus splice β-variant; GenBank accession number AF333984). The domains of Fe65 that bind to the cytoplasmic tail of APP or to Tip60 were studied by quantitative yeast two-hybrid assays (*22*), which demonstrated that the first PTB domain of Fe65 is necessary and sufficient for binding to

Tip60, and the second PTB domain, for binding to APP. For Tip60, both a partial rat cDNA and full-length human cDNA were analyzed (*22*).

29. J. Kamine, B. Elangovan, T. Subramanian, D. Coleman, G. Chinnadurai, *Virology* **216**, 357 (1996).
30. Q. Ran, O. M. Pereira-Smith, *Gene* **258**, 141 (2000).
31. T. Yamamoto, M. Horikoshi, *J. Biol. Chem.* **272**, 30595 (1997).
32. T. Ikura *et al.*, *Cell* **102**, 463 (2000).
33. The GST pull-down assays were performed essentially as described (*46*), by using purified wild-type and mutant rat GST-Tip60β, APP, and Myc-Fe65 expressed by transfection in COS cells. Extracts from transfected COS cells were incubated for 4 hr at 4°C with 10 μg of GST-Tip60 or GST-Tip60* bound to glutathione agarose. Beads were washed five times in 0.15 M NaCl, 50 mM Hepes-NaOH, pH 7.5, 1% IGEPAL CA-630 (Sigma) resuspended in 100 μl SDS-polyacrylamide gel electrophoresis (SDS-PAGE) sample buffer, and 20 μl were analyzed by SDS-PAGE and immunoblotting using antibodies to APP and the HA- and Myc-epitopes.
34. C. Zwahlen, S. C. Li, L. E. Kay, T. Pawson, J. D. Forman-Kay, *EMBO J.* **19**, 1505 (2000).
35. C. Dalluin *et al.*, *Mol. Cell* **6**, 921 (2000).
36. Y. Yan, N. A. Barlev, R. H. Haley, S. L. Berger, R. Marmorstein, *Mol. Cell.* **6**, 1195 (2000).
37. HeLa cells plated on cover glass in a 12-well plate were transfected with pcDNA3.1-N-HA-Fe65, pCMVMyc-hTip60, and pCMV5-APP (0.2 μg each) using Fugene6 (Roche). Two days after transfection, cells were washed two times with PBS, fixed (3.7% formaldehyde for 10 min at room temperature), and blocked and permeabilized in PBS containing 3% bovine serum albumin, 0.1% IGEPAL CA-630 for 20 min. Cells were then incubated with mouse monoclonal antibody against HA (BabCo, Berkeley, CA), rabbit polyclonal antibody against APP, and goat polyclonal antibody against Myc (Santa Cruz Biotechnology, Santa Cruz, CA) for 1 hour, washed three times with PBS, and treated with the appropriate Cy2-, Cy3-, and Cy5-labeled secondary antibodies (Jackson Laboratories) for 1 hour. After three washes with PBS and one wash with water, cells were mounted and observed by microscopy.
38. G. Minopoli *et al.*, *J. Biol. Chem.* **276**, 6545 (2001).
39. For transactivation assays of Gal4-Tip60, COS, HeLa, and HEK293 cells were cotransfected with one of the following: (i) pG5E1B-luc (Gal4 reporter plasmid); (ii) pCMV-LacZ (β-galactosidase control plasmid); (iii) pMst (Gal4); pM-hTip60 (full-length wild-type human Gal4-Tip60β); or pM-hTip60* (full-length mutant human Gal4-Tip60β); (iv) pCMV5-Fe65 (Fe65), pCMVMyc-Fe65(242-711) [Fe65(242-711)], pCMV5-Fe65(1-553) (Fe65Δ PTB2), or pCMV5-Fe65mW4 (Fe65mW4) where indicated; and (v) pCMV5-APP (human APP695) or pCMV5-APP* (mutant human APP695). All transfections contained one of the plasmids listed in (i to iii), whereas (iv) and (v) were variable. Analyses were performed as described in (*19*).
40. M. S. Brown, J. Ye, R. B. Rawson, J. L. Goldstein, *Cell* **100**, 391 (2000).
41. Y. M. Chan, Y. N. Jan, *Cell* **94**, 423 (1998).
42. B. L. Sopher *et al.*, *Brain Res. Mol. Brain Res.* **26**, 207 (1994).
43. D. C. Lu *et al.*, *Nature Med.* **6**, 397 (2000).
44. A. B. Vojtek, S. M. Hollenberg, J. A. Cooper, *Cell* **74**, 205 (1993).
45. M. Okamoto, T. C. Südhof, *J. Biol. Chem.* **272**, 31459 (1997).
46. Y. Hata, C. A. Slaughter, T. C. Südhof, *Nature* **366**, 347 (1993).
47. X. Cao, T. Südhof, unpublished observations.
48. We thank C. Haass (Munich, Germany), N. Huang and W. Miller (UCSF), R. Roeder (Rockefeller University), J. Herz, E. Olson, J. Lu, M. Lush (University of Texas, Southwestern), K. Beyreuther (Heidelberg, Germany), and R. Jahn (Goettingen, Germany) for reagents and advice. We are grateful to S. Sisodia, M. S. Brown, J. L. Goldstein, E. H. Koo, and D. Selkoe for advice and discussions.

4 January 2001; accepted 29 May 2001

A Neural Correlate of Working Memory in the Monkey Primary Visual Cortex

Hans Supèr,[1,2]* Henk Spekreijse,[1] Victor A. F. Lamme[1,2]

The brain frequently needs to store information for short periods. In vision, this means that the perceptual correlate of a stimulus has to be maintained temporally once the stimulus has been removed from the visual scene. However, it is not known how the visual system transfers sensory information into a memory component. Here, we identify a neural correlate of working memory in the monkey primary visual cortex (V1). We propose that this component may link sensory activity with memory activity.

We trained monkeys (*Macaca mulatta*) to perform a delayed-response task in which the animals had to remember briefly the location of a figure after it had been removed from the visual scene (*1*). The animals fixated on a small central red dot on a computer screen (Fig. 1). After a 300-ms fixation, a motion-defined figure appeared very briefly (28 ms) at one of three locations (Fig. 1). After this stimulus had been presented, the animal had to continue fixating the central spot until it was switched off (Fig. 1A, "Cue time"). The removal of the fixation point indicated to the animal to make a saccade toward the position where the figure had been presented. The animal was rewarded only when fixation was maintained until the cue, and when the saccade was made to the correct position. The latency of the cue time was varied between 0 and 2000 ms after stimulus onset. Thus, while fixating, the animal had to remember the location of the briefly presented figure during a period of up to about 2 s. Detection of the figure was high and declined for longer delay periods (Fig. 2A), indicating that the task requires short-term memory processes.

During the delayed-response task, multiunit activity of V1 neurons was recorded in two monkeys (*2*). The display was filled with random dots. Stimulus onset thus evoked neural responses for "figure" [when the figure dots were overlying the V1 receptive fields (RFs)] as well as for "ground" motion (when the figure was presented elsewhere and background dots covered the RF) (Fig. 1C). We arranged the directions of motion such that, on average, the motion stimuli on the RF were identical for the "figure" and "ground" situations (*3*, *4*).

The initial responses to figure and ground motion were identical up to about 70 ms after stimulus onset (Fig. 2B). At longer latencies, however, the response to figure motion was typically stronger than to background motion. This late enhancement of the sensory response—contextual modulation—correlates closely with the perception of the figure (*4*–*6*). Contextual modulation in V1 depends on feedback from higher visual areas (*7*–*9*), which implies that it is a specific correlate of recurrent processing. What happens to this modulation once the stimulus is no longer present, but has to be remembered?

During the delay period, the figure response remained stronger than the ground response (Fig. 2B) ($P < 10^{-4}$ for all delay periods). Thus, contextual modulation continues after the figure is removed from the visual field. In a control experiment, we observed the same phenomenon when a static, rather than a moving, stimulus was used in the same delayed-response task. Here, a static texture with an orientation-defined figure (*10*) was presented for 100 ms and followed by a mask containing a different texture, where the figure was no longer visible. Also in this experiment, contextual modulation continued during the whole period (900 ms) that the animal had to remember the figure location (Fig. 2E). Thus, the persistence of contextual modulation is not due to any peculiarity of the motion stimulus.

We calculated the strength of contextual modulation (*3*) for the first 250 ms after stimulus onset as an indication of the initial segregation strength of the figure from ground, and for the last 250 ms before cue time as an indication of the signal strength available for responding in the memory task. In the first part of the response, the strength of contextual modulation was similar for all

---

[1] Graduate School Neurosciences Amsterdam, Department of Visual System Analysis, Academic Medical Center, University of Amsterdam, Post Office Box 12011, 1100 AA Amsterdam, Netherlands. [2] The Netherlands Ophthalmic Research Institute, Meibergdreef 49, 1105 BA Amsterdam, Netherlands.

*To whom correspondence should be addressed. E-mail: h.super@ioi.knaw.nl